

Anisotropic softening of collective charge modes in the vicinity of critical doping in a doped Mott insulator

Y.W. Li,¹ D. Qian,¹ L. Wray,¹ D. Hsieh,¹ Y. Kaga,² T. Sasagawa,² H. Takagi,²
R.S. Markiewicz,³ A. Bansil,³ H. Eisaki,⁴ S. Uchida,² and M.Z. Hasan¹

¹*Department of Physics, Joseph Henry Laboratories of Physics, Princeton University, Princeton, NJ 08544*

²*Department of Physics, University of Tokyo, Tokyo 113-8656, Japan*

³*Department of Physics, Northeastern University, Boston, MA 02115*

⁴*AIST, 1-1-1 Central 2, Umezono, Tsukuba, Ibaraki, 305-8568 Japan*

(Dated: November 7, 2018)

Momentum resolved inelastic resonant x-ray scattering is used to map the evolution of charge excitations over a large range of energies, momenta and doping levels in the electron doped Mott insulator class $\text{Nd}_{2-x}\text{Ce}_x\text{CuO}_4$. As the doping induced AFM-SC (antiferromagnetic–superconducting) transition is approached, we observe an anisotropic softening of collective charge modes over a large energy scale along the $\Gamma \rightarrow (\pi, \pi)$ -direction, whereas the modes exhibit broadening (~ 1 eV) with relatively little softening along $\Gamma \rightarrow (\pi, 0)$ with respect to the parent Mott insulator ($x=0$). Our study indicates a systematic collapse of the gap consistent with the scenario that the system dopes uniformly with electrons even though the softening of the modes involves an unusually large energy scale.

PACS numbers: 78.70.Ck, 71.20.-b, 74.25.Jb

The evolution of a strongly correlated material with doping—from a Mott insulator to a conducting metal—is one of the most intensively studied issues in current condensed matter physics. This fascinating evolution has proven to be full of surprises such as the appearance of high- T_c superconductivity, non-Fermi liquid behavior, and nanoscale phase separation [1]. Mott insulators often exhibit phase transitions upon doping, which are signaled or hallmarked by the softening of collective charge or spin modes. The behavior of spin modes has been investigated extensively via neutron scattering [2]. Although charge excitations near the Brillouin zone (BZ) center can be accessed by optical techniques [3], their behavior with momentum over the full BZ remains largely unexplored. Here, as demonstrated in recent experimental [4, 5] and theoretical studies [6, 7], inelastic x-ray scattering indeed provides such a unique opportunity.

While previous studies have focused largely on either the undoped 1-D [8] or 2-D [4, 5] insulators, or the hole-doped superconductors [9], Mott insulators can be doped with electrons as well. In fact, it appears that with electron doping bands in the cuprates evolve in a much more straightforward and systematic manner [10, 11, 12, 13, 14] than with hole doping. However, a direct study of the doping induced changes in the collective excitation spectra of a Mott insulator is lacking. Previous x-ray scattering work [15] focused on the highly electron doped *superconductor* (SC) $\text{Nd}_{1.85}\text{Ce}_{x=0.15}\text{CuO}_4$, observed intraband and interband excitations and interpreted the excitations in a one-band model with long-range hoppings. However, Ref[15] does not report the undoped Mott insulator and the way gap modes of the Mott insulator are related to the doping where superconductivity sets in. In this Letter, we report a high-

resolution study of how the collective charge excitations of the Mott insulating state ($x=0$) develop with electron doping in approaching the critical AFM-SC transition (before reaching the optimal doping) for the first time. Our finding, made possible by studying the insulating states, is that, as the electron-doping induced AFM-SC transition is approached from the $x=0$ Mott side, the system exhibits an anisotropic softening of excitations over a large energy scale (~ 5 eV) along the $\Gamma \rightarrow (\pi, \pi)$ -direction, whereas the modes exhibit broadening (~ 1 eV) with relatively little softening along $\Gamma \rightarrow (\pi, 0)$. Our results suggest that a multi-orbital Hubbard model is essential to describe the observed evolution from the $x=0$ Mott state in contrast to the 1-band model with long-range hoppings proposed in Ref[15] based on the superconductor only. Moreover, our results show that the *evolution* of Mott physics of the electron-doped cuprate is dramatically different from that reported in the hole-doped cuprates [9].

The electronic structure of $\text{Nd}_{2-x}\text{Ce}_x\text{CuO}_4$ (NCCO) has been studied by angle-resolved photoemission (ARPES) and optical spectroscopies. ARPES studies [16] find that the electrons dope directly into the bottom of the upper Hubbard band and yield small Fermi (FS) pockets, with a crossover around optimal doping to a large FS. Such a scenario, where the magnetic order remains commensurate without signs of ‘stripe’ (charge inhomogeneity) or other phase separation, also describes magnetization[13, 17, 18] and optical data[19].

The experiments were performed at CMC-CAT beamline 9-ID-B at the Advanced Photon Source. Resonant inelastic x-ray scattering (RIXS) at copper K edge allows a large enough momentum transfer to cover several BZ’s. The scattered photon energy was measured by using a

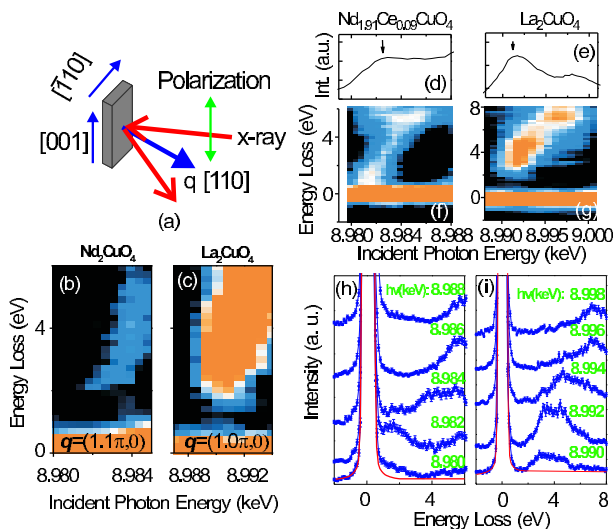


FIG. 1: Incident energy dependence of electronic excitations: (a) Vertical scattering geometry employed with x-ray field along [001]. (b) and (c) X-ray energy dependence of inelastic excitations for Nd_2CuO_4 and La_2CuO_4 . Q -values are chosen to minimize large quasielastic background. (d)–(g) Excitations near the Mott gap are seen to be enhanced near the first absorption peak, not only in the undoped insulator, but also in the doped system. A few energy-loss curves corresponding to the data images in (f) and (g) are shown in (h) and (i). The red curves show the fits to the quasielastic data.

diced Ge (733) crystal analyzer, and the intensity was recorded by a solid state detector. The overall energy resolution was set to about 0.37 eV in order to *improve count* efficiency, enabling us to detect fine momentum-dependent details of the spectra. All data are taken at room temperature. To avoid possible polarization induced artifacts when measuring the in-plane anisotropy, the sample was mounted with incident polarization directed along the c -axis (Fig.1(a)). The data were collected at several values of the momentum transfer vector $\mathbf{q} = \mathbf{k}_i - \mathbf{k}_f$ in the 2nd BZ along the [100] direction, and in the 4th BZ along the [110] direction. The coupling to various excitations in the x-ray scattering process, near a resonance, depends in general on the energy of the incident photons. Accordingly, we first examined the detailed incident energy dependence of the loss spectra at several momenta. Representative data sets are presented in Fig. 1. It is known that the charge-transfer gap excitations resonate near the first absorption peak [9]. Similar resonance behavior is seen in Nd_2CuO_4 , which is like that in the more extensively studied $\text{La}_{2-x}\text{Sr}_x\text{CuO}_4$ [9]. However, the scattering intensity at the low-energy branch is about an order of magnitude *weaker*. Our systematic investigations summarized in Fig. 1 show that similar shape of the resonance profile is seen for the lower energy excitations in the electron doped system. Accordingly, we employed the photon energy of 8.982 keV (this energy is above the $1s \rightarrow 3d$ edge which suppresses the

crystal-field excitations [20] as it is not the focus of the current study). Therefore, in the theoretical simulations such incident energy correspondences of the excitation spectra are maintained for comparison with the measured data.

Fig.2 summarizes our RIXS data on NCCO. In the undoped system in panel (a), a broad excitation is observed near the zone center around 2 eV with an onset energy of ≈ 1 eV, which is consistent with the charge transfer gap found in this compound in optical studies [21]. It is seen to lose intensity as it approaches the zone corner along the $[\pi, \pi]$ as well as the $[\pi, 0]$ directions (Fig.2(a)). Along $[\pi, \pi]$, it merges at the zone corner with a higher excitation band near 5 eV which disperses upward. With doping these two high energy branches split at (π, π) as seen in (b) and (c), but only the lower energy branch softens significantly (i.e. moves to lower energy), so that the overdoped system in (c) displays a large excitation gap at the (π, π) point from 2 eV to 4 eV. In sharp contrast, the aforementioned 2 eV branch evolves uniformly along $[\pi, 0]$, and softens rapidly near the zone center as it tends to close the excitation gap with doping. Notably, the zero-loss energy is not accessible due to the presence of the strong quasielastic peak (see, e.g., Fig.1(h)), making it difficult to extract significant data below ≈ 0.4 eV, where fitting and subtraction of the quasielastic peak lead to uncertainties. Nevertheless, the softening of the low energy excitations is evident in the data over the BZ.

The preceding observations are further highlighted through the directly measured data curves presented in Fig.3. Doping dependent changes in the individual energy-loss curves are compared in (a). Along [110], doping splits the peak in the undoped spectrum around 5 eV at (π, π) (red uppermost curve on the left side of (a)) into two peaks, and the lower of these peaks softens rapidly with doping. In contrast, along [100] a monotonic softening of the low energy excitations is found. Changes in the positions of various spectral features and some of the associated leading edges are plotted in (b) as a function of momentum and doping. The upper branches around 5-6 eV are seen to be affected weakly by doping. Despite a significant softening of one of the modes around (π, π) , the closing of the excitation gap is limited to the region of the zone center as one approaches the superconducting phase ($x = 0.14$). These results are in clear contrast to the behavior in hole-doped cuprates such as the $\text{La}_{2-x}\text{Sr}_x\text{CuO}_4$ or the $\text{YBa}_2\text{Cu}_3\text{O}_{7+d}$ series[9].

Recent theoretical analyses [7, 15] of data on $x=0.15$ samples suggest two different scenarios. The analysis of the data using a 1-band model Ref[15] suggests a no gap collapse scenario whereas the analysis of high doping data in Ref.[7] suggests a gap collapse scenario. Which of these two opposite viewpoints is correct cannot be ascertained from the data of Ref.[15] alone. Therefore it is crucial to study the evolution of the undoped compound of this series with high resolution so that the low-energy gap

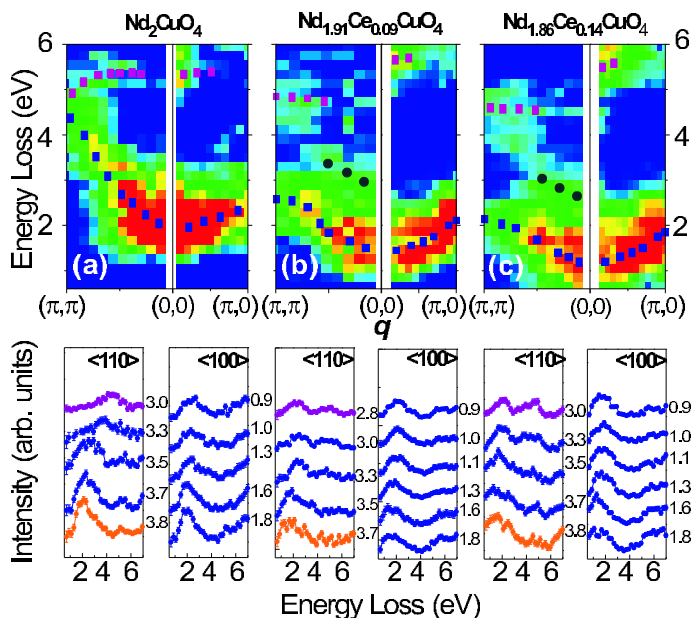


FIG. 2: Doping evolution of charge excitations in NCCO. (a) $x=0$ (parent Mott state), (b) $x=0.09$ (doped AFM), and (c) $x=0.14$ (superconductor). Upper row shows intensity maps in the reduced-zone using a color scheme where high intensity is denoted by red and low by blue. Black, grey and red dots are guides to the eye for the dispersion of low, medium and high energy excitation branches, respectively. Lower row gives a few representative spectra corresponding to the images in the upper row. Absolute momentum values (in units of π/a_0) are shown attached to various spectra and lie in the 4th BZ along $\langle 110 \rangle$ and the 2nd BZ along $\langle 100 \rangle$.

excitations can be accessed and model the evolution of the spectra from the $x=0$ Mott side. To interpret the present data in terms of RIXS spectra computed within the framework of a three-band Hubbard Hamiltonian of NCCO, based on Cu $d_{x^2-y^2}$ and two O p_σ orbitals, we extend the theoretical framework described in [7] by incorporating the doping evolution data made available here for the first time. The specific values of the parameters used in this work to fit the spectra are: $t_{\text{CuO}} = 0.85$ eV, $t_{\text{OO}} = -0.6$ eV, $\Delta_0 = -0.3$ eV, $U_p = 5.0$ eV; where t_{CuO} and t_{OO} are the Cu-O and O-O nearest neighbor (NN) hopping parameters, n_d [n_p] is the average electron density on Cu [O], m_d the average electron magnetization on Cu, and U [U_p] is the Cu [O] on-site Coulomb repulsion. The remaining parameter, crucial for *fitting the doping evolution of the excitations*, the Hubbard U , is taken to be 7.45 eV at $x=0$ with weak doping dependence: $U=6.69$ eV at $x=0.09$ and $U=6.27$ eV at $x=0.14$, so that the effective U decreases by about 16% over this doping range, reflecting presumably the effects of screening. We note that before proceeding with RIXS computations, we determined the chemical potential and the magnetization m_d on Cu sites self-consistently at each doping level. m_d values so found are: 0.32 at $x=0$; 0.19

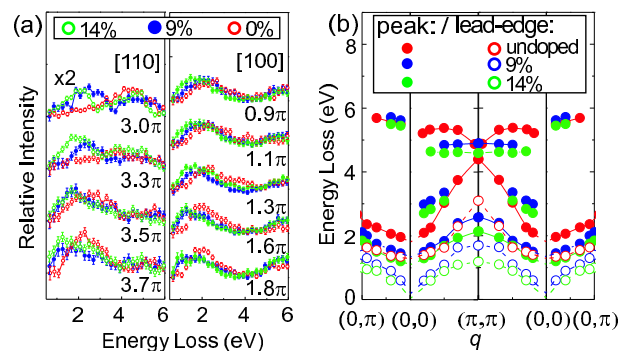


FIG. 3: (a) Spectral curves (raw data) along $\langle 110 \rangle$ and $\langle 100 \rangle$ for the undoped system (red points) are compared at various momenta with the corresponding spectra for the doped system (black and green points). (b) Positions of peaks (marked in Fig.-2(a-c)) based on the center of gravity method [4, 8] of various spectral features (filled circles) and some of the associated leading edges (open circles) as a function of momentum and doping are plotted.

at $x=0.09$; and 0.12 at $x=0.14$.

Figure 4 (top) shows the calculated RIXS intensity maps. The positions of various experimentally observed spectral peaks (filled circles) and the leading edge of the low energy feature (filled diamonds) are superposed for ease of comparison. The high energy peaks involve transitions from the nonbonding O and bonding Cu-O bands to unoccupied states in the antibonding band, and fall in the same energy range as transitions involving other Cu and O orbitals not included in the present 3-band model. Therefore, it is appropriate to concentrate on the behavior of RIXS peaks within a few electron volts, which are associated with the antibonding Cu-O band, split by AFM ordering. In this energy region the theoretically predicted changes in the energies of various features as a function of momentum and doping are in reasonable accord with experimental observations highlighted in the discussion of Figs.2 and 3 above. In particular, the softening of low energy peaks is well reproduced and the collapse of the gap occurs only near Γ in the computations. The latter effect can be readily understood. The RIXS transitions involve both intraband and interband contributions. In the absence of a gap, only *intraband* transitions are possible near Γ which can only exist near zero energy transfer close to the Fermi level. Away from Γ , intraband transitions can take place at finite energies, but when a gap opens up, *interband* transitions become allowed, *even at Γ* [23].

Although the computed maps in the top row of Fig.4 are shown unbroadened to highlight spectral features, the theoretical spectra shown in the bottom panels of Fig.4 (blue lines) have been smoothed to mimic the broadening of experimental lineshapes[22]. The relative intensities of the computed peaks are seen to be in agreement with our experimental results in lower energies[24], excepting

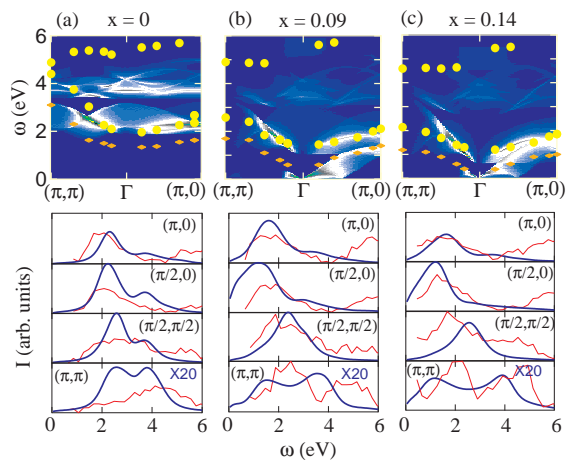


FIG. 4: *Top row*: Doping evolution of RIXS spectra obtained within a three-band Hubbard model as a function of energy transfer ω at momenta \mathbf{q} along Γ to (π, π) and $(\pi, 0)$ directions for three different dopings x . Positions in $\omega - \mathbf{q}$ space of various experimentally observed spectral peaks (filled circles) and the leading edge of the low energy feature (filled diamonds) are superposed. Computed spectra have not been broadened to reflect experimental resolution in order to highlight spectral features. *Bottom row*: Comparison of theoretical (blue lines) and experimental (red lines) spectra. Three columns refer to the three indicated doping levels x . Each column includes four different q -values as shown; experimental spectra are at the closest q -value measured. Theoretical spectra have been smoothed to reflect experimental broadening[22].

the momentum region near the (π, π) -point, where both the experimental and theoretical intensities are weak, but the computed cross-section is smaller. A similar behavior is seen in the $\text{La}_{2-x}\text{Sr}_x\text{CuO}_4$ series [9]. Excitonic effects associated with longer range Coulomb coupling (intersite- V) beyond that included in our model computations could enhance and redistribute spectral weight near zone boundaries [25]. The *low-energy, gap-edge* dispersion relations (E vs. q) are in agreement as seen from the top row of Fig-4(a-c)[23].

Taken together, these results suggest that the parent $x=0$ Mott insulating state of NCCO is doped uniformly by the addition of electrons (within the resolution) and that the AFM-gap collapses near the onset of the SC phase as seen from the systematics in Fig.5. In Fig.5(b) we plot the doping dependence of the leading-edge gap (edge, green squares) and peak position (peak, white diamonds) of the lowest branch at Γ . [Since quasielastic scattering makes it difficult to obtain experimental data right at Γ , these values are found by extrapolation from nearby points, as shown in Fig.5(c).] Within the experimental uncertainties the gap collapses in the vicinity of the Γ -point as one approaches the critical doping regime in the phase diagram. For comparison, we also show in Fig.5(b) $\Delta_m = Um_d$, the AFM-correlation gap[7, 10] based on our present calculation (filled circles) and the

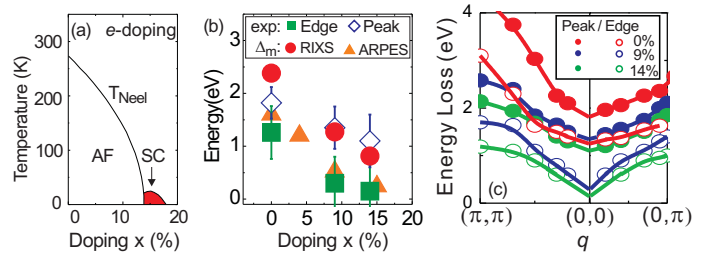


FIG. 5: (a) Schematic temperature-doping ($T - x$) phase diagram of NCCO. (b) The leading-edge gap (green squares) and peak positions (white diamonds) of the lowest energy excitation branch in RIXS data at the Γ -point are compared with AFM correlation gap Δ_m from the present calculation (filled circles) and from ARPES (triangles)[10] as a function of doping. (c) The excitation modes (branches) are fitted and extrapolated to the Γ -point(0,0) based on the branch curvatures, to extract the data points presented in (b). Peak position are shown in the raw data in Fig-2(a-c) and leading-edges are from data in Fig-3.

corresponding ARPES[10, 26] results (triangles), which are seen to be in agreement. In general, our analysis suggests that the anisotropic softening involving a large energy scale observed near the Mott insulating state requires going beyond the one band model.

In summary, we have utilized the unique momentum resolution of x-ray scattering to map the evolution of particle-hole excitations in the electron doped cuprate from its parent Mott state ($x=0$) to the doping on-set for superconductivity. We observe a nearly degenerate charge excitation mode near the (π, π) point around 5 eV in the Mott insulator, which splits on doping away from half-filling, with its lower energy branch softening anisotropically in approaching the AFM-SC critical doping. In contrast, the response near the $(\pi, 0)$ wavevector exhibits damping with relatively little softening. Our results indicate a systematic collapse of the gap consistent with the scenario of *uniform doping* when electrons are added into the parent Mott state which is in clear contrast to what is reported in *hole-doped* Mott insulators where charge inhomogeneity is commonly observed. The unusual softening of the modes from the Mott state likely contributes to many unusual behaviors of cuprates.

We acknowledge T. Gog and D. Casa for technical assistance. This work is primarily supported by DOE/DE-FG02-05ER46200. Use of the Adv. Photon Source was supported by DOE/W-31-109-Eng-38. The theoretical part of the work is supported by the US Department of Energy contracts DE-AC03-76SF00098 and DE-FG02-07ER46352, and benefited from the allocation of super-computer time at the NERSC and Northeastern University's Advanced Scientific Computation Center (ASCC).

-
- [1] M. Imada *et al.*, Rev. Mod. Phys. **70**, 1039 (1998).
- [2] M.A. Kastner *et al.*, Rev. Mod. Phys. **70**, 897 (1998).
- [3] G. Blumberg *et al.*, Science **278**, 1427 (1997).
- [4] Y.-J. Kim *et al.*, Phys. Rev. Lett. **89**, 177003 (2002); M.Z. Hasan *et al.*, Science **288**, 1811 (2000).
- [5] J.P. Hill *et al.*, Phys. Rev. Lett. **80**, 4967 (1998); C. C. Kao *et al.*, Phys. Rev. B **54**, 16361 (1996); P. Abbamonte *et al.*, Phys. Rev. Lett. **83**, 860 (1999).
- [6] K. Tsutsui *et al.*, Phys.Rev.Lett. **83**, 3705 (1999); T. Devereaux *et al.*, Phys.Rev.Lett. **90**, 067402 (2003); T. Nomura, J. Igarashi, Phys.Rev.B **71**, 035110 (2005); J.v.d. Brink, M.v. Veenendaal, Europhys.Lett., **73** 121 (2006).
- [7] R.S. Markiewicz *et al.*, Phys.Rev.Lett. **96**, 107005 (2006).
- [8] M.Z. Hasan *et al.*, Phys.Rev.Lett. **88**, 177403 (2002).
- [9] K. Ishii *et al.*, Phys. Rev. Lett. **94**, 187002 (2005); Y.-J. Kim *et al.*, Phys. Rev. B **70**, 094524 (2004).
- [10] C. Kusko *et al.*, Phys. Rev. B **66**, 140513 (2002).
- [11] H.Kusunose, T.M. Rice, Phys.Rev.Lett.**91**,186407(2003).
- [12] D. Sénéchal *et al.*, Phys. Rev. Lett. **92**, 126401 (2004).
- [13] B. Kyung *et al.*, Phys. Rev. Lett. **93**, 147004 (2004).
- [14] Q. Yuan *et al.*, Phys. Rev. B **72**, 054504 (2005).
- [15] K. Ishii *et al.*, Phys. Rev. Lett. **94**, 207003 (2005).
- [16] N.P. Armitage *et al.*, Phys. Rev. Lett. **88**, 257001 (2002).
- [17] H. J. Kang *et al.*, Nature **423**, 522 (2003); P. Mang *et al.*, Phys. Rev. Lett. **93**, 027002 (2004).
- [18] R.S. Markiewicz, Phys. Rev. B **70**, 174518 (2004).
- [19] A. Zimmers *et al.*, cond-mat/0510085 (2005).
- [20] J.W. Seo *et al.*, Phys. Rev. B **73**, 161104 (2006).
- [21] Y. Tokura *et al.*, Phys. Rev. B **41**, 11657 (1990).
- [22] The spectra were first smoothed with a Gaussian of 0.37 eV width to account for the resolution. The spectra were further smoothed via folding with a Lorentzian of 0.30 eV width to mimic what appears to be an intrinsic linewidth.
- [23] The branch near 4 eV is weak in the experimental data. Since this branch has a different symmetry than the 2 eV branch it resonates at a different photon energy (near 8.894 eV) as evident from the raw data profile in Fig-1(f).
- [24] The experimental spectra for energy transfers beyond about 6 eV contain significant contributions from bands beyond the 3-band model we considered for this work.
- [25] K. Penc and W. Stephan, Phys. Rev. B **62**, 12707 (2000).
- [26] In the one-band model, U has a different definition, and the magnetic gap is $\Delta_m = 2Um_d$. Also, at $x=0$, ARPES does not see the upper band giving a lower limit to Δ_m .